ELSEVIER

Biophysical Chemistry 116 (2005) 23–31

Biophysical Chemistry

http://www.elsevier.com/locate/biophyschem

Dynamics of proteins and lipids in the stratum corneum: Effects of percutaneous permeation enhancers

Sheila Gonçalves do Couto, Matheus de Souza Oliveira, Antonio Alonso*

Instituto de Física, Universidade Federal de Goiás, Goiânia 74001-970, GO, SP, Brazil

Received 10 October 2004; received in revised form 26 January 2005; accepted 26 January 2005
Available online 4 February 2005

Abstract

We have spin labeled the stratum corneum (SC) with a lysine specific reagent, succinimidyl-2,2,5,5-tetramethyl-3-pirroline-1-oxyl-carboxylate spin label (SSL), to assess the dynamics and hydration degree of SC proteins by electron paramagnetic resonance (EPR) spectroscopy taking measurements directly from the intact tissue. Treating the SC with two percutaneous penetration enhancers, 8 M urea or 20% (v/v) *1*-methyl-2-pyrrolidone (1 MP), destabilizes the proteins thus promoting more mobile and solvent-exposed protein conformations. Upon SC lipid depletion the nitroxide side chain becomes more solvent exposed, suggesting that the removal of hygroscopic substances in the extraction process favors more hydrated protein conformations. On the other hand, the treatments with 8 M urea or 40% (v/v) 1 MP did not alter significantly the fluidity in the SC lipid domain as assessed by the probe 5-doxyl stearic acid; these permeation enhancers, specially 1 MP, seem to increase the probe solubility in the solvent leading to a considerable fraction of spin label to be removed from the lipid domain.

Keywords: Stratum corneum; EPR; Spin label; Protein mobility; BSA; Urea and pyrrolidone

1. Introduction

The outermost layer of the epidermis, SC, plays an important role as a low-permeability membrane that controls transepidermal water loss and the permeation of solutes in both directions across skin. The SC cells–keratin-filled corneocytes–contain a ~15 nm thick layer of protein assembly, called the cornified cell envelope, formed just inside the plasma membrane as the cells terminally differentiate [1,2]. The cell envelope is highly insoluble as a result of extensive cross-linking of intermolecular disulfide bonds and isopeptide bonds between glutamine and lysine residues of neighboring polypeptides catalyzed by calcium-dependent transglutaminases present in the keratinocyte membrane [3]. The outer surface of the cell envelope consists of a 5 nm-thick monomolecular layer of long-chain ω-hydroxyceramides, covalently linked by an ester bond, which forms the corneocyte lipid envelope [4,5]. The corneocytes are separated by highly ordered lipid lamellae, consisting primarily of ceramides, cholesterol and saturated fatty acids [6]. It has been proposed that the protein-bonded ceramides interdigitate with intercellular lipids, forming a scaffold for the organization and stability of the intercellular lamellae [7]. The envelope proteins cannot be isolated, which prevents a direct analysis; however, at least 20 envelope proteins have been identified in many studies through immunoelectron microscopy, using antibodies to known precursor proteins from the epidermis [8].

Despite scientific effort, the molecular architecture of SC and the mechanisms that control the transepidermal water loss or influence the permeation of solute through the skin are not yet well understood. Information about the molecular organization of SC is important for the treatment

Abbreviations: SC, stratum corneum; BSA, bovine serum albumin; EPR, electron paramagnetic resonance; SSL, succinimidyl-2,2,5,5-tetramethyl-3-pirroline-1-oxyl-carboxilate; 5-DSA, 5-doxyl stearic acid; 16-DSA, 16-doxyl stearic acid; 1 MP, 1-methyl-2-pyrrolidone; NLLS, nonlinear least-squares fitting program.

* Corresponding author. Fax: +55 62 521 1014.
E-mail address: alonso@fis.ufg.br (A. Alonso).

0301-4622/$ - see front matter © 2005 Elsevier B.V. All rights reserved.
doi:10.1016/j.bpc.2005.01.009

of skin diseases, percutaneous drug delivery and the cosmetic maintenance of the skin [9].

EPR spectroscopy of proteins spin-labeled at lysine residues has been employed to assess mobility and conformational changes of proteins [10,11]. The EPR spectra of spin-labeled protein are generally composed of basically two motional components, which are technically called strongly (S) and weakly (W) immobilized components, relative to the timescale of EPR experiments with nitroxides. In earlier studies [12–14] based on careful line-shape simulations, these two components were found to result from a thermodynamic equilibrium between two nitroxide populations, which differ essentially in the mobility states. The less mobile spectral component arises when the nitroxide side chain adopts a "bent" conformation on the lateral polypeptide chain, forming a hydrogen bond between the nitroxide-oxygen atom and the protein (rigid structure), whereas spin-labeled chains whose nitroxide moieties are in contact with the solvent provide the more mobile component. In addition, the changes in standard Gibbs free energy, enthalpy and entropy involved in the conversion between these two components were calculated [14].

In this work, we present evidences that corroborate a new interpretation of the EPR spectra of nitroxide linked to proteins, analyzing by line-shape simulations the dynamics and conformational changes caused by SC-lipid depletion or treatment of SC with urea or 1 MP. Furthermore, the effects of these two permeation enhancers on the protein and lipid components of SC are compared.

2. Materials and methods

2.1. Spin labeling of intact and lipid-depleted SC and albumin

SC membranes were obtained from newborn Wistar rats less than 24 h old and were prepared as described elsewhere [12,13]. A piece of SC (~1 mg) was incubated for 1 h at 24 °C in 100 μl of buffered saline (100 mM $NaHCO_3$, 150 mM NaCl and 1 mM EDTA, pH 8.3) and 10 μl of DMSO with 5 mg/ml of SSL, purchased from Molecular Probes (Eugene, OR). The SC membrane was dried on filter paper and incubated in ~2 ml of buffer under moderate agitation for 2 min in each of five successive washings to eliminate free unbound label. The spin labels 5- and 16-doxyl stearic acid (5- and 16-DSA) having the nitroxide radical moiety (doxyl) at the 5th, and 16th carbon atom of the acyl chain, respectively, were purchased from Sigma Chem. Co. (St. Louis, MO) and the SC was spin labeled as described elsewhere [15–17]. The sample was introduced into a capillary tube for EPR measurements and, under these conditions, was considered to be in a fully hydrated state, with a water content of 58±7% (g of H_2O/g of wet SC). EPR measurements were performed at pH 5.1, approximately the pH found on the skin surface [18], in acetate buffered saline (10 mM acetate, 150 mM NaCl and 1 mM EDTA). Treatments with urea or 1 MP were performed incubating the spin-labeled SC for 1 h with 8 M urea or 2 h with 20% (v/v) 1 MP. The newborn rat SC was lipid-depleted following the method used by Wertz and Downing [4] for porcine SC. A sheet of SC (~2 mg) was incubated for 1-h intervals in each of three successive extraction mixtures (~1.5 ml) of chloroform/methanol (2:1, 1:1 and 1:2, v/v). This extraction procedure was repeated, changing the solvents at 2-h intervals, followed by a 2 h extraction in methanol. Bovine serum albumin (BSA; Sigma Chem. Co., St. Louis, MO) at 0.2 mM was incubated at ~4 °C for 24 h in phosphate-buffered saline (10 mM phosphate, 150 mM NaCl and 1 mM EDTA, pH 7.4) with 10 μl of DMSO containing 5 mg/ml of SSL. To remove the free spin label, the albumin was dialyzed for ~24 h at ~4 °C against the phosphate-buffered saline.

2.2. EPR spectroscopy

A Bruker ESP 300 spectrometer equipped with the ER 4102 ST resonator and operating at X-band (9.4 GHz) was utilized in our investigations. The parameters of the spectra used were microwave power, 20 mW; modulation frequency, 100 KHz; modulation amplitude, 1.024 G; magnetic field scan, 100 G; sweep time, 168 s and detector time constant, 41 ms. Temperature was controlled within 0.3 °C by the nitrogen stream system (Bruker, Rheinstetten, Germany). EPR spectral simulations were performed using a nonlinear least-squares (NLLS) fitting program developed by Freed and coworkers [19]. The program is based on the stochastic Liouville equation [19,20] and allows for fitting a single spectrum with two components having different mobility and magnetic tensor parameters, giving the relative populations and the associated rotational correlation times. The magnetic g and A tensors are fixed in the nitroxide moiety. By convention, the x-axis points along the N–O bond, the z-axis is parallel to the 2pz axis of the nitrogen atom, and the y-axis is perpendicular to x and z [19,20]. The constants of rotational diffusion rates around the x, y and z-axis are also defined in this molecule-fixed frame. The laboratory frame is defined with the z-axis along the magnetic field. Based on the stochastic Liouville theory the program monitors the transformation between two frames, which is modulated by the nitroxide motions. The program allows to take into account local ordering described by a restoring potential that is defined relative to a local director frame, but whose directors are isotropically distributed so that there is no macroscopic ordering [19,20]. In practice, better fittings are obtained adjusting two parameters, denoted c20 and c22, which determine the strength and the asymmetry of the potential, respectively. The input parameters of tensors g and A (G) used for two-spectral components, here called S and W components, are listed in Table 1. These parameters were determined based on a general analysis of the overall spectra obtained in this work

Table 1
Principal components of the magnetic tensors g (g-factor) and A (hyperfine splitting) used in the nonlinear least-squares fitting program (NLLS)

Parameter	Component 1	Component 2
g_{xx}	2.0098	2.0073
g_{yy}	2.0057	2.0050
g_{zz}	2.0026	2.0026
A_{xx} (G)	6.0	5.0
A_{yy} (G)	6.9	5.0
A_{zz} (G)	37.4	34.0

and, once determined, all the EPR spectra were simulated using the same pre-established values.

3. Results

3.1. EPR spectra of spin-labeled proteins

Fig. 1a shows the experimental and best-fit EPR spectra at 2 °C of spin-labeled lysine residues of SC tissue. The EPR spectra of spin-labeled proteins are composed of basically two spectral components, indicating that the spectrum consists of two fractions of spin probes with very different states of mobility. By line-shape simulation, using a two-components model with one fast and one slow rotational correlation times, it was possible to separate these components, the strongly (S) and weakly (W) immobilized components (Fig. 1b and c). The fraction of most mobile spin labels has rotational correlation times on the nanosecond scale and an isotropic hyperfine splitting, $2a_0$, consistent with spin labels in buffer (17.1±0.5 G). Hyperfine coupling $2a_0$ is very sensitive to the solvent polarity where the nitroxide moiety is dissolved, so that, the observed value assures that the nitroxide radicals from the component W are all exposed to solvent. The component strongly immobilized on the 9.4 GHz EPR timescale for the nitroxide radical (Fig. 1c) has a rotational diffusion rate about one order of magnitude lower than that of component W, evidencing the strong interactions of the nitroxide side chain with the protein backbone.

The population ratio of the strongly and weakly immobilized components, N_s/N_w, in the composite spectrum diminishes with increasing temperature and, since this process is completely reversible, these two motional components are clearly in thermodynamic equilibrium. In previous work [12–14] this phenomenon has been interpreted as arising from two interchangeable nitroxide states: bonded (S) and non-hydrogen bonded (W) to the protein. In Fig. 2, a molecular model illustrates the possible formation

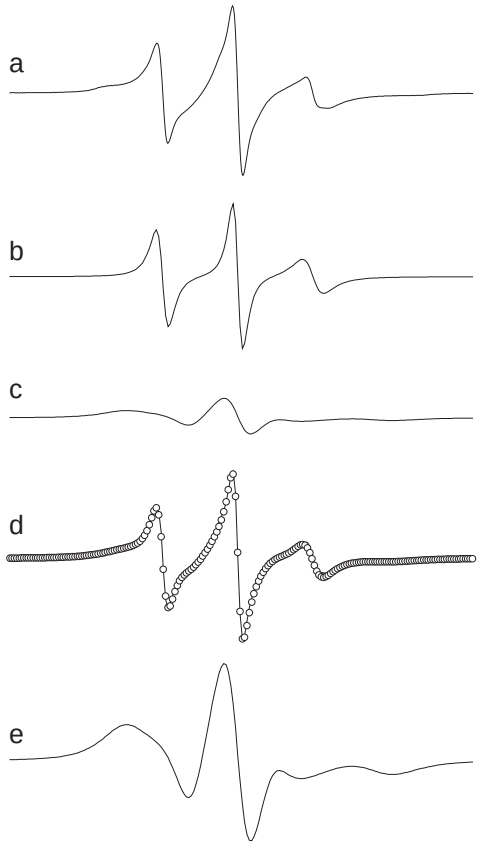

Fig. 1. (a) Experimental EPR spectra at 2 °C of spin label SSL covalently bound to lysine residues of the stratum corneum in acetate buffered saline pH 5.1. (b) and (c) Calculated weakly (W) and strongly (S) immobilized components, respectively. The best-fit spectra in this study were obtained by NLLS fit, using a two-component model for all fits. (d) Experimental (line) and simulated (empty circles) EPR spectra. (e) The amplified strongly immobilized component. The EPR parameters $2a_0$, isotropic hyperfine splitting, and $2T'_{//}$, the outer hyperfine splitting, are indicated. Range of magnetic field scans: 100 G.

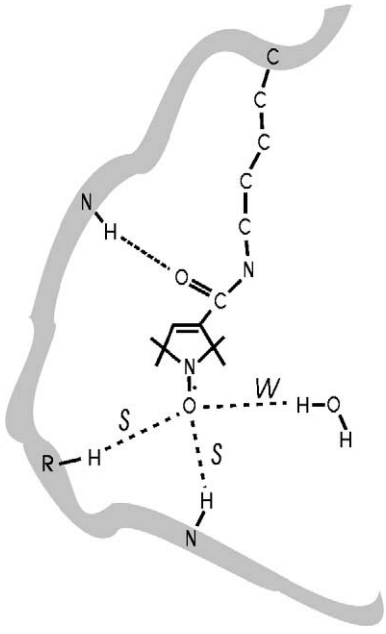

Fig. 2. Schematic molecular model illustrating the spin label SSL bound to the lysine lateral chain. The nitroxide moiety can form hydrogen bonds either with the protein (amide groups or lateral chains of the residues), generating the strongly immobilized component (S), or with the water to generate the weakly immobilized component (W). Also indicated is a possible hydrogen bond between the oxygen atom from the nitroxide side chain and the local polypeptide chain.

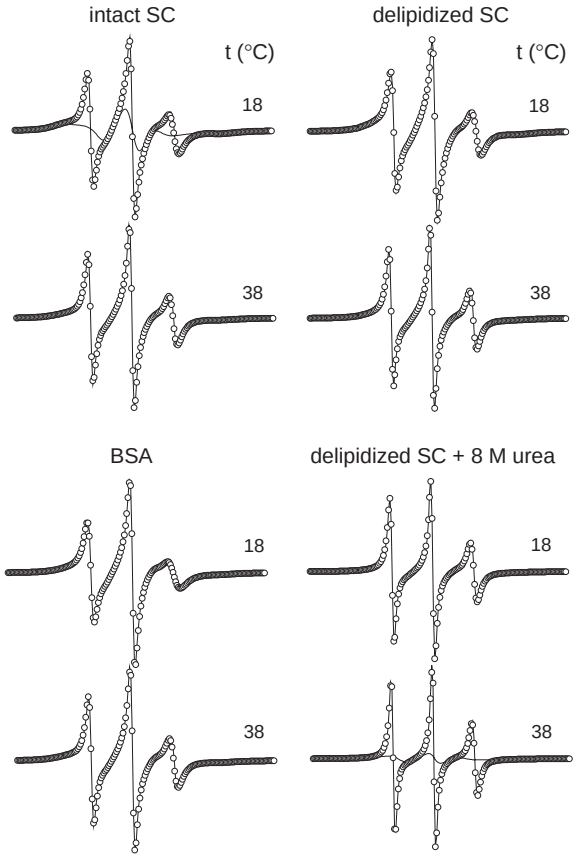

Fig. 3. Experimental (lines) and best-fit (empty circles) EPR spectra at 18 and 38 °C of SSL attached to intact stratum corneum (pH 5.1), lipid depleted stratum corneum in the absence and in the presence of 8 M urea (pH 5.1) and bovine serum albumin (pH 7.4). The less mobile component (S) is also presented for the first and the last spectrum. Range of magnetic field scans: 100 G.

of hydrogen bonds of spin label SSL with a generic segment of polypeptide chain.

3.2. Protein mobility of SC decreases in presence of urea

Fig. 3 shows a series of experimental and simulated EPR spectra of SSL bound to SC or BSA at two temperatures. The relative populations of the two fractions of radicals, as well as the apparent motional parameters R_{bar}S (component S) and R_{bar}W (component W), can be obtained [19,20] in each spectral simulation. The NLLS fitting program can be used to calculate the rotational diffusion tensor, i.e., it determines the rotational motion in each component of a molecule-fixed frame [19,20]. However, to simplify the operational aspects of the program dealing with two spectral components simultaneously, and to obtain a more accurate result, we used only the R_{bar}S and R_{bar}W parameters, which represent mean values of rotational rates for each component. We assume an axially symmetric rotational diffusion tensor with $R_{bar}=(R_{\perp}^2.R_{//})^{1/3}$ and a rotational anisotropy with $R_{//}=10\ R_{\perp}$ [20]. As shown in Fig. 3, the convergences were very good.

Fig. 4 presents the population ratio of the spin labels in the two dynamic states as a function of the reciprocal temperature. The plots for the samples of intact and delipidized SC and BSA showed a linear behavior throughout the range of measured temperatures. At higher temperatures, and especially in the case of the urea-treated samples, the W-population was very high and the fitting program failed to successfully describe the experimental spectra with the used model. Considerable increases in the ratio N_w/N_s were observed for the samples treated with 8 M urea and a more discrete increase was observed when the intact SC was

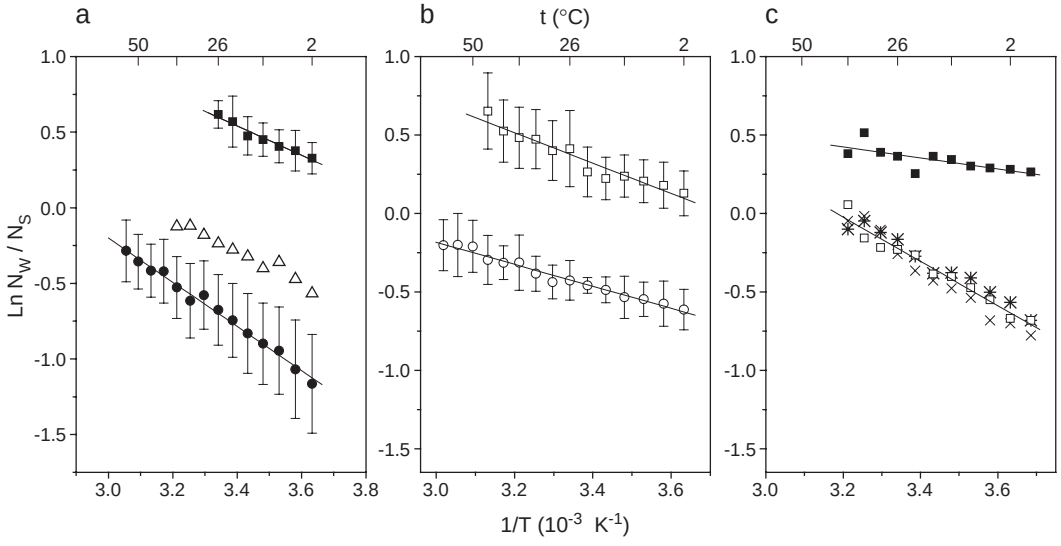

Fig. 4. van't Hoff graph. The natural logarithm of the population ratio between weakly and strongly immobilized components, N_w/N_s, in the EPR spectra of spin label SSL attached to proteins as a function of the reciprocal absolute temperature. Panels: (a) intact stratum corneum; (b) lipid-depleted stratum corneum; and (c) bovine serum albumin. Symbols: circles (control for stratum corneum), open triangles [20% (v/v) *1*-methyl-2-pyrrolidone], squares (8 M urea), stars and crosses (control for albumin), open squares (albumin with 2 M urea).

Table 2
Changes in standard Gibbs free energy (at 26 °C), enthalpy and entropy to associate the nitroxide side chain to polypeptide chain in stratum corneum (SC) or BSA

Samples	$\Delta G^{o}_{W\rightarrow S}$ kcal mol^{-1}	$\Delta H^{o}_{W\rightarrow S}$ kcal mol^{-1}	$\Delta S^{o}_{W\rightarrow S}$ cal mol^{-1} K^{-1}
Intact SC	−0.42±0.14[a]	−2.91±0.52	−8.36±1.26
+8 M urea	0.36±0.07	−1.93±1.15	−7.66±4.00
+20% (v/v)1 MP	−0.14	−2.05	−6.40
Lipid-depleted SC	−0.25±0.07	−1.40±0.49	−3.83±1.80
+8 M urea	0.22±0.10	−1.93±0.57	−7.22±2.17
BSA	−0.13	−2.82	−8.98
+8 M urea	0.22	−0.70	−3.09

The proteins were spin-labeled with the lysine-specific reagent SSL.
[a] The numerical values were calculated based on Eq. (3) and on data from the van't Hoff graph (Fig. 4).

treated with 20% (v/v) 1 MP. It is worth noting that all the EPR spectra were completely reversible; after the measurement was performed up to the higher temperatures, each sample was measured again at 38 °C to check the reversibility.

Considering that the spin-label population ratio, N_w/N_s, is given by the Boltzmann distribution with only two energy levels and that each level contains n states of degeneracy, or n ways to obtain that energy level, an expression for the population ratio can be written [21].

$$N_w = n_w/n_s N_s \exp[-(E_w - E_s)/RT] \quad (1)$$

or

$$\ln N_w/N_s = \ln n_w/n_s - (E_w - E_s)/RT, \quad (2)$$

where n_w/n_s is a pre-exponential factor that reflects the ratio of the number of configurations that form W and S components, and E_w and E_s are the energies of the probe in contact with the water and protein, respectively.

N_w/N_s is the ratio of spin labels at equilibrium, ΔG=0, and

$$\ln N_w/N_s = \ln K = -\Delta G^{\circ}/RT = \Delta S^{\circ}/R - \Delta H^{\circ}/RT, \quad (3)$$

where K is the equilibrium constant, ΔS^{o} is the entropy change (=R ln n_w/n_s) and ΔH^{o} is the enthalpy change in the equilibrium state. Because the equilibrium tends towards the formation of S-component at low temperatures, one finds that $E_w > E_s$ and that the system reduces its free energy in the W→S direction. Eq. (3) shows that, in practice, the numerical values of ΔS^{o} and ΔH^{o} can be determined from a plot, called a van't Hoff graph, such as the one presented in Fig. 4. The slope coefficient should give $-\Delta H^{o}/R$ and the intercept should yield $\Delta S^{o}/R$ (sense: S→W). Table 2 presents the calculated values of $\Delta G^{o}_{W\rightarrow S}$ (at 26 °C), $\Delta H^{o}_{W\rightarrow S}$ and $\Delta S^{o}_{W\rightarrow S}$ for the samples of intact and delipidized SC and BSA. It must be emphasized that we assume a non-coupled equilibrium where there is no variation in the heat capacity between the two states of the nitroxide side chain (ΔC_p=0); hence, ΔH^{o} should not vary with T. This assumption seems true, considering the linear behavior displayed in the curves of the van' t Hoff graphs (Fig. 4). Our findings show that, when the temperature increases, the system absorbs heat and becomes less organized; in other words, the conversion from S to W is an endothermic process accompanied by an entropy increase. The difference in enthalpy is also the apparent energy required to dissociate the motionally restricted nitroxide moiety from protein backbone and the change in entropy is the increment of disorder or motion received by the nitroxide side chain. Thus, in the presence of urea or 1

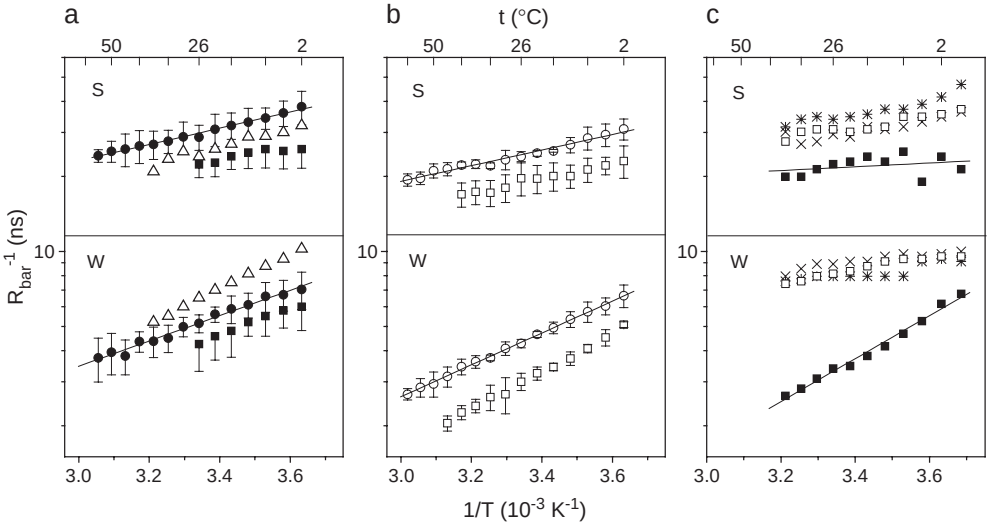

Fig. 5. Effective rotational correlation times for the strongly $(R_{bar}S)^{-1}$ and weakly $(R_{bar}W)^{-1}$ immobilized components as a function of the reciprocal absolute temperature. The $R_{bar}S$ refers to the local motions in the protein backbone and the $R_{bar}W$ to the rotational motions of the nitroxide side chain. The parameters were obtained from the spectral fittings of SSL EPR spectra in intact stratum corneum (panel a), lipid-depleted stratum corneum (panel b) or in bovine serum albumin (panel c). Symbols: circles (control for stratum corneum), open triangles [20% (v/v) *1*-methyl-2-pyrrolidone], squares (8 M urea), stars and crosses (control for albumin), open squares (albumin with 2 M urea).

MP, the S↔W equilibrium tends towards the formation of the component W, which represents a configuration of greater energy or less stability.

Fig. 5 shows the rotational motion parameters $(R_{bar}S)^{-1}$ and $(R_{bar}W)^{-1}$ provided by the fittings of the EPR spectra as a function of the reciprocal absolute temperature. $(R_{bar}S)^{-1}$ reflects the segmental motion of the backbone, since the spin labels of the component S are tethered in the protein, whereas $(R_{bar}W)^{-1}$ reflects the rotational motion of the nitroxide side chain in the aqueous phase and can therefore be affected by the micro-viscosity in the vicinities of the lysine residues. As can be seen, both parameters were quite sensitive to temperature and the urea treatment increased the rotational correlation time for the three samples. The permeation enhancer 1 MP increased the motion of the protein backbone ($R_{bar}S$) but constrained the motion of the spin-labeled side chain free in the solvent ($R_{bar}W$).

To examine if urea and 1 MP modify the SC-lipid dynamics, we spin labeled the SC with the membrane probes 5- and 16-DSA as in previous studies [15–17]. The EPR spectra of 5-DSA shown in Fig. 6 indicated that the treatments of SC with 40% 1 MP or 8 M urea did not alter significantly the lipid fluidity. The spin label 16-DSA did not also show alterations in the lipid fluidity for both treatments (this is shown in Fig. 6 just for the treatment with urea). However, the EPR spectra showed that both compounds alter the solvent properties increasing its capacity in dissolving the fatty-acid spin probes

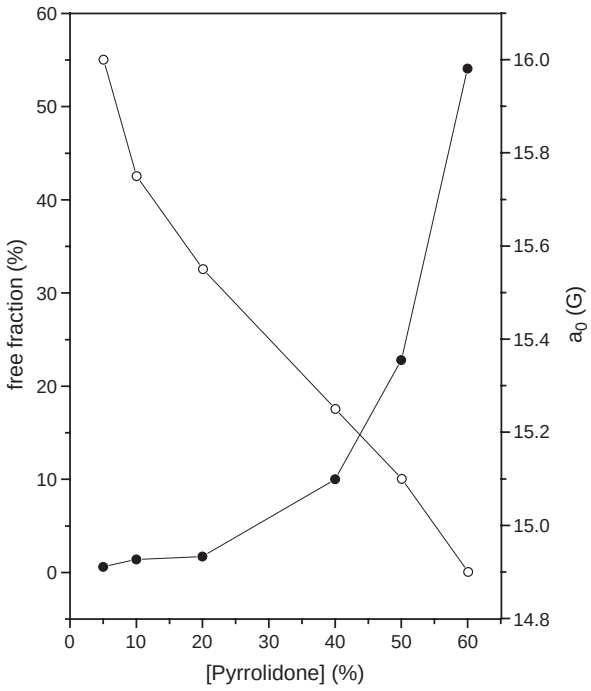

Fig. 7. Fraction of free component (spin label free in the solvent) (circles) and the isotropic hyperfine splitting, $2a_0$ (open circles), in the EPR spectra of 5-doxyl stearic acid in stratum corneum at 26 °C and pH 5.1, as a function of the *1*-methyl pyrrolidone (1 MP) concentration (%, v/v). The free fraction was obtained with NLLS fit program (see spectrum b from Fig. 6). The $2a_0$, an EPR parameter sensible to the solvent polarity, was measured directly in the experimental spectra.

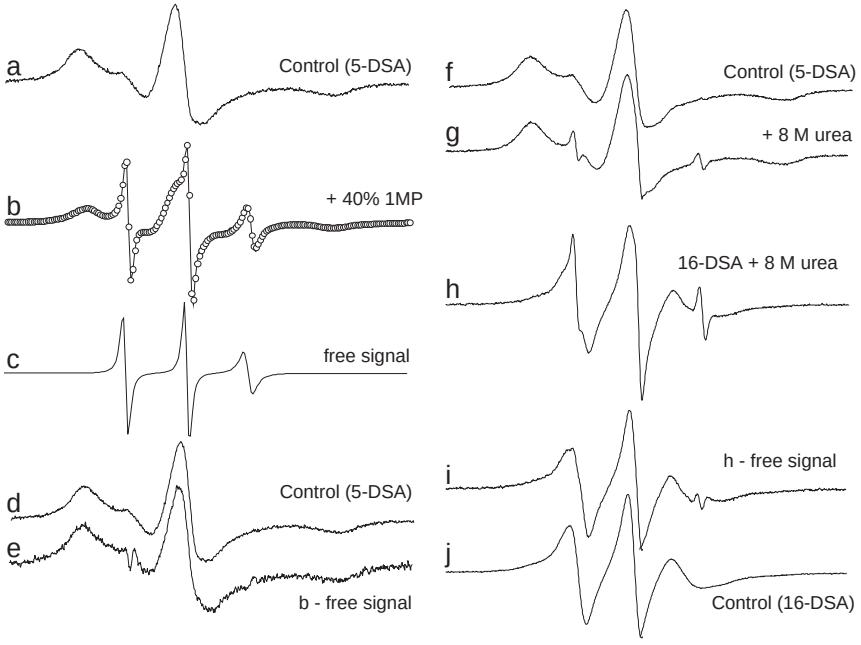

Fig. 6. EPR spectra of stearic acid derivatives spin labels (5- and 16-DSA) in stratum corneum (pH 5.1) at 26 °C. (a) Control for 5-DSA, (b) the SC was treated with 40% (v/v) *1*-methyl-2-pyrrolidone (1 MP); the best-fit spectrum (empty circles) was obtained by NLLS fit, using a simulation model with two spectral components, (c) the best-fit spectrum of the free component (spin labels free in the solvent), (d) control for 5-DSA, (e) spectrum b with the free component (spectrum c) subtracted, (f) the control for 5-DSA again, (g) the 5-DSA in stratum corneum treated with 8 M urea, (h) the 16-DSA in stratum corneum with 8 M urea, (i) spectrum h with the free component subtracted, and (j) the control for 16-DSA. The total scan ranges of the magnetic field were 100 G.

derivatives. Fig. 7 shows that the solvent polarity decreases and the amount of spin labels free in the solvent increases with the pyrrolidone concentration. For 60% pyrrolidone the EPR spectra indicated that more than half of the spin probes left the SC lipid domain. In the case of urea this effect is less pronounced: at 8 M less than 5% of the spin labels were dislocated from the SC membranes.

4. Discussion

4.1. Thermodynamic parameters of a nitroxide side chain and the analysis of proteins

We have determined the thermodynamic profile of a nitroxide side chain by measuring the temperature dependence of the equilibrium constant for two nitroxide states, known as the van't Hoff method. For a recent discussion about the concerns involving the application of this method, see the work of Horn and co-workers [22], in which the authors have compared the enthalpy, ΔH^{o}, determined directly by calorimetry and indirectly by the van' t Hoff method, finding no discrepancies when all the variables of the system were allowed to equilibrate with temperature. However, large contributions of heat capacity change, ΔC_p, can be observed in the presence of linked equilibria. The linear behavior of all the curves in the van't Hoff graph (Fig. 4) indicates that this method is applicable to our system.

Urea and 1 MP increased the Gibbs potential difference $\Delta G^{o}_{W\rightarrow S}$ (Table 2) in the samples of intact and delipidized SC and BSA, stabilizing the interaction of the lysine-bound SSL with the solvent (the proportion of component W with higher energy is greater).

In lipid depleted SC the lysine-bound probe was more solvent-exposed. The delipidization process also removes hygroscopic substances of the natural moisturizing factor of SC, such as free amino acids, organic acids, urea and inorganic ions [23], and the lack of these osmolytes may increase the osmotic pressure on the proteins, increasing their hydration degrees. Finally, the free-energy parameter also indicated that the SSL side chain was more exposed to the solvent in BSA solution than in SC tissue.

The $\Delta H^{o}_{W\rightarrow S}$-variations could be rationalized based in the results of a previous work [14], which showed increases of $\Delta H^{o}_{W\rightarrow S}$ with the dehydration of SC. The $\Delta H^{o}_{W\rightarrow S}$-values of spin label SSL decreased with the SC-delipidization process, suggesting a more effective contact of the probe with the bulk water, which has a higher water activity, or capacity to dissolve the nitroxide side chain. Urea possibly affects the changes in enthalpy by two compensatory effects: (i) causing protein expansion, it increases the contact with the bulk water, increasing the local solvent activity, which, in turn, reduces the enthalpy and, in contrast, (ii) urea at 8 M may, itself, reduce the solvent activity. In intact SC, the increase in the local solvent activity prevailed, due to protein expansion, while in delipidized SC, where the $\Delta H^{o}_{W\rightarrow S}$ was already low, the presence of urea increased the enthalpy to the level of intact SC treated with urea, suggesting that 8 M urea can recover the solvent activity to levels that correspond to those provided by the natural moisturizing factor.

The most interesting feature of the EPR spectra of spin-labeled protein is that they normally allow one to calculate the rotational correlation time for two independent situations: (i) the side chain motions, $(R_{bar}W)^{-1}$, reflecting essentially an effective correlation time due to rotational isomerizations around the bonds that link the nitroxide ring to the protein, and ii) the segmental motions of the polypeptide chains, $(R_{bar}S)^{-1}$, that reflects the local fluctuations or torsional oscillations about backbone dihedral angles since the nitroxide side chain is strongly coupled to the polypeptide chain in this case. Urea increased the overall diffusional rates for both types of motion in the three measured samples. The increase in the local backbone motion may have resulted from exposure to water or expansion of the protein due to hydration of hydrophobic groups, and this may also have contributed to the increase observed in the rotational motion of the more free spin-labeled chain, since the structure on the point of attachment was more mobile in the presence of urea. Upon lipid-depleting SC, the two parameters indicated small increases of motional dynamics, probably as a consequence of removing the natural moisturizing factor of SC (free amino acids, organic acids, urea and inorganic ions [23]), providing a more effective contact between proteins and the bulk water.

Weber and co-workers [24] demonstrated that urea decreases the pressure that produces a given degree of virus dissociation. The dissociation of oligomeric proteins into subunits by hydrostatic pressure indicates that the separated solvated subunits occupy a smaller volume than the original aggregate [24,25]. The authors attributed this effect of progressive destabilization to direct protein–urea interactions rather than to an indirect effect on the solvent, which would produce the opposite effect. Interestingly, many small organic osmolytes, such as the naturally occurring solute trimethylamine-*N*-oxide, counteract the actions of urea on proteins, having the property of protecting intracellular proteins against the denaturation and loss of functional activity caused by urea [26–28]. It has been proposed that urea loosens and expands protein volume, decreasing its functional activity, while trimethylamine-*N*-oxide increases protein activity by shifting its conformation towards the most compact and active form [26]. The effects of urea and trimethylamine-*N*-oxide are both related to the influence of these solutes on solvation; thus, a poorer solvent than water, generally associated with organic compounds, will compete with water for the formation of hydrogen bonds with the protein and favor more compact and less exposed protein conformations. Because urea in aqueous solutions is a better solvent than water in the sense that it can form hydrogen

bonds with the protein, enhancing protein hydration, it will favor more expanded and exposed protein configurations [28].

4.2. Lipid-depletion and penetration enhancers effects on SC

Our research group has investigated previously SC proteins spin labeled with maleimide derivative spin labels [12–14], which are specific for sulfhydryl groups, and in the present work SC proteins were spin-labeled with the succinimidyl derivative, SSL, specific for Lys [10,11]. The $\Delta G^{o}_{W\rightarrow S}$ and $\Delta H^{o}_{W\rightarrow S}$-values for SH groups (−1.0 and −6.4 Kcal/mol, respectively [14]) are consistent with less solvent-exposed nitroxides. Two non-equivalent SH groups are present in SC: those localized in the corneocyte envelope are more reactive than the ones located inside the corneocyte, which are characterized by a nitroxide side chain more exposed to the solvent. Using EPR signal intensity it was estimated that a maximum of about 2 nmol of maleimide spin label are bound per milligram of newborn rat SC [12,13]. Amounts of 8.1% Cys and 2.5% Lys have been reported for the cornified cell envelope of newborn mouse epidermis [29] and of 3.1% Cys and 4.7% Lys for the entire pig SC [30]. In the current work an accurate evaluation of the amount of labeled Lys in SC was not performed, but it seems to be similar to that of free SH groups. To confirm that the spin label SSL does not react with the SH groups of SC, we performed experiments blocking these sites with *N*-ethyl-maleimide before the spin labeling. Blocking the SH-groups prevents the modification with the maleimide but not with the succinimide label. In spite of the complexity of SC as a biological system and the fact that only an unspecific labeling of a determined residue can be made, EPR spectroscopy seems promising for learning more about the structure and dynamics of this system.

In SC, the activities of urea have been ascribed to its capacity to bind with proteins, causing swelling of the tissue and reducing its barrier-like property [31]. Urea is considered a hydrating agent used in the treatment of scaling conditions such as psoriasis and ichthyosis [32]. EPR spectra of spin probes 5- and 16-DSA showed that the treatments with 8 M urea or 40% 1 MP do not change the SC-lipid dynamics significantly. The single significant change in the EPR spectra was that both 1 MP and urea-treated samples always displayed a fraction of free spin labels, suggesting that these compounds create domains of interstitial water in SC, which are able to accommodate these hydrophobic nitroxides. In the case of the pyrrolidone this effect is critical at high concentrations (about 50%), because the solvent acquires a very high capacity to sequestrate the lipids from the membranous structures. Urea is considered a skin penetration enhancer of the amides chemical class for hydrophilic drugs [33], but, when combined with alkanols or polyethylene glycol, it can also accelerate permeation of hydrophobic drugs such as progesterone and indomethacin [34,35]. Since urea does not significantly alter the order and mobility of the SC lipids, its action should result only from interactions with proteins. Pyrrolidones have been used as penetration enhancers in human skin for hydrophilic (e.g. mannitol, 5-fluorouracil and sulphaguanidine) and lipophilic (betamethasone-17-benzoate, hydrocortisone and progesterone) permeants [32]. In contrast with the treatment with urea the pyrrolidone derivative analyzed here presented moderate effects on protein mobility. Urea hydrates and expands the SC proteins but, at low concentrations, it also has a minor and opposite effect as a component of the natural moisturizing factor [23], i.e., urea also exerts an indirect effect as an osmolyte that reduces the water activity in the tissue or the osmotic pressure on the proteins, stabilizing more compact and less hydrated conformations. At higher concentrations, however, urea causes a great increase in molecular dynamics and excessive SC hydration, which explains its action as a permeation enhancer for drug delivery through the skin.

Acknowledgements

This work was supported by a grant from CNP_q (Conselho Nacional de Desenvolvimento Científico e Tecnológico) to A. A. (300908/92-0), by master fellowships from CAPES (Coordenação de Aperfeiçoamento de Pessoal de Nível Superior) to S.G.C. and M.S.O., and by supports from CNPq (472273/2003-5), FUNAPE (Fundação de Apoio à Pesquisa-UFG), PROINPE (Programa Goiano de Incentivo à Pesquisa), and Fundação de Amparo à Pesquisa do Estado de São Paulo (FAPESP), all Brazilian institutions. The authors are grateful to the Dr. Marcel Tabak (IQSC) for valuable discussions.

References

[1] Z. Nemes, P.M. Steinert, Bricks and mortar of the epidermal barrier, Exp. Mol. Med. 31 (1999) 5–19.
[2] P.M. Steinert, L.N. Marekov, Initiation of assembly of the cell envelope barrier structure of stratified squamous epithelia, Mol. Biol. Cell 10 (1999) 4247–4261.
[3] J.L. Abernethy, R.L. Hill, L.A. Goldsmith, Epsilon-(gamma-glutamyl)lysine cross-links in human stratum corneum, J. Biol. Chem. 252 (1977) 1837–1839.
[4] P.W. Wertz, D.T. Downing, Covalently bound ω-hydroxyacylsphingosine in the stratum corneum, Biochim. Biophys. Acta 917 (1987) 108–111.
[5] M. Behne, Y. Uchida, T. Seki, P.O. Montellano, P.M. Elias, W.M. Holleran, Omega-hydroxyceramides are required for corneocyte lipid envelope (CLE) formation and normal epidermal permeability barrier function, J. Invest. Dermatol. 114 (2000) 185–192.
[6] G.M. Gray, R.J. White, H.J. Yardley, Lipid composition of the superficial stratum corneum cells of the epidermis, Br. J. Dermatol. 106 (1982) 59–63.
[7] D. Hohl, Cornified cell envelope, Dermatologica 180 (1990) 201–221.

[8] P.M. Steinert, The complexity and redundancy of epithelial barrier function, J. Cell Biol. 151 (2000) F5–F7.
[9] S.H. White, D. Mirejovsky, G.I. King, Structure of lamellar lipid domains and corneocyte envelopes of murine stratum corneum, Biochemistry 27 (1988) 3725–3732.
[10] R.J. Singh, J.B. Feix, H.S. Mchaourab, N. Hogg, B. Kalyanaraman, Spin-labeling study of the oxidative damage to low-density protein, Arch. Biochem. Biophys. 320 (1995) 155–161.
[11] A. Kostrzewa, T. Páli, W. Froncisz, D. Marsh, Membrane location of spin-labeled cytochrome c determined by paramagnetic relaxation agents, Biochemistry 39 (2000) 6066–6074.
[12] A. Alonso, J.G. Santos, M. Tabak, Stratum corneum protein mobility as evaluated by a spin label maleimide derivative, Biochim. Biophys. Acta 1478 (2000) 89–101.
[13] A. Alonso, W.P. Santos, S.J. Leonor, J.G. Santos, M. Tabak, Stratum corneum protein dynamics as evaluated by a spin label maleimide derivative. Effect of urea, Biophys. J. 81 (2001) 3566–3576.
[14] A. Alonso, J.V. Silva, M. Tabak, Hydration effects on the protein dynamics in stratum corneum as evaluated by EPR spectroscopy, Biochim. Biophys. Acta 1646 (2003) 32–41.
[15] A. Alonso, N.C. Meirelles, M. Tabak, Lipid chain dynamics in stratum corneum studied by spin label electron paramagnetic resonance, Chem. Phys. Lipids 104 (2000) 101–111.
[16] A. Alonso, N.C. Meirelles, M. Tabak, Effect of hydration upon the fluidity of intercellular membranes of stratum corneum: an EPR study, Biochim. Biophys. Acta 1237 (1995) 6–15.
[17] A. Alonso, N.C. Meirelles, V.E. Yushmanov, M. Tabak, Water increases the fluidity of intercellular membranes of stratum corneum: correlation with water permeability, elastic, and electrical properties, J. Invest. Dermatol. 106 (1996) 1058–1063.
[18] E. Berardesca, F. Pirot, M. Singh, H. Maibach, Differences in stratum corneum pH gradient when comparing white and black African-American skin, Br. J. Dermatol. 139 (1998) 855–857.
[19] D.J. Schneider, J.H. Freed, Spin labeling: theory and application, in: L.J. Berliner, J. Reuben (Eds.), Biological Magnetic Resonance, vol. 8, Plenum Press, New York, 1989, pp. 1–76.
[20] D.E. Budil, S. Lee, S. Saxena, J.H. Freed, Nonlinear-least-squares analysis of slow-motion EPR spectra in one and two dimensions using a modified Levenberg–Marquardt algorithm, J. Magn. Reson., Ser. A 120 (1996) 155–189.
[21] K.E. van Holde, W.C. Johnson, P.S. Ho, Principles of Physical Biochemistry, Prentice-Hall, New Jersey, 1998.
[22] J.R. Horn, J.F. Brandts, K.P. Murphy, Van't Hoff and calorimetric enthalpies: II. Effects of linked equilibria, Biochemistry 41 (2002) 7501–7507.
[23] Y. Jokura, S. Ishikawa, H. Tokuda, G. Imokawa, Molecular analysis of elastic properties of the stratum corneum by solid-state ^{13}C-nuclear magnetic resonance spectroscopy, J. Invest. Dermatol. 104 (1995) 806–812.
[24] G. Weber, A.T. Da Poian, J.L. Silva, Concentration dependence of the subunit association of oligomers and viruses and the modification of the latter by urea binding, Biophys. J. 70 (1996) 167–173.
[25] J.L. Silva, G. Weber, Pressure stability of proteins, Annu. Rev. Phys. Chem. 44 (1993) 89–113.
[26] T. Mashino, I. Fridovich, Effects of urea and trimethylamine-*N*-oxide on enzyme activity and stability, Arch. Biochem. Biophys. 258 (1987) 356–360.
[27] P.H. Yancey, G.N. Somero, Methylamine osmoregulatory solutes of elasmogranch fishes counteract urea inhibition of enzymes, J. Exp. Zool. 212 (1980) 205–213.
[28] I. Baskakov, A. Wang, D.W. Bolen, Trimethylamine-*N*-oxide counteracts urea effects on rabbit muscle lactate dehydrogenase function: a test of the counteraction hypothesis, Biophys. J. 74 (1998) 2666–2673.
[29] A.C. Steven, P.M. Steinert, Protein composition of cornified cell envelopes of epidermal keratinocytes, J. Cell Sci. 107 (1994) 693–700.
[30] O. Lopes, A. de la Maza, L. Coderch, J.L. Parra, Study of the composition and structure of pig stratum corneum based on the action of different solubilizing agents, Colloids Surf., A Physicochem. Eng. Asp. 123–124 (1997) 415–424.
[31] S.K. Han, Y.H. Jun, Y.J. Rho, S.C. Hong, Y.M. Kim, Percutaneous absorption-enhancing activity of urea derivatives, Arch. Pharm. Res. 14 (1991) 112–118.
[32] A.C. Williams, B.W. Barry, Penetration enhancers, Adv. Drug Deliv. Rev. 56 (2004) 603–618.
[33] B.W. Barry, Novel mechanisms and devices to enable successful transdermal drug delivery, Eur. J. Pharm. Sci. 14 (2001) 101–114.
[34] T. Nishihata, J.H. Rytting, A. Kamada, K. Matsumoto, K. Takahashi, Combined effect of alcohol and urea on the in vitro transport of indomethacin across rat dorsal skin, J. Pharm. Sci. 79 (1990) 487–489.
[35] C. Valenta, S. Wedenig, Effects of penetration enhancers on the in-vitro percutaneous absorption of progesterone, J. Pharm. Pharmacol. 49 (1997) 955–959.